

Thermal Spike Model of Track Formation in $\text{YBa}_2\text{Cu}_3\text{O}_{7-x}$

B.F. Kostenko, J. Pribiš

Laboratory of Information Technologies, JINR

With the miniaturization of technologies enabling nano dimensions ion track engineering takes now on special significance. Particularly, latent swift heavy ion tracks in high- T_c superconductors are able to act as vortex pinning centers and to increase dramatically the critical current density of the materials. At present no satisfactory theory of track formation in high- T_c superconductors exists in spite of the manifest practical importance of this application. Theoretically, several different mechanisms, among which is the thermal spike (TS), are possible. According to the TM model, the material melts within a cylinder along the trajectory of an energetic ion if the temperature exceeds the melting point. Subsequent fast cooling down leads to amorphous phase formation in place of melted one, i.e. to latent track constitution.

The first TM description of track formation in high- T_c superconductors neglected latent heat of melting and, therefore, predicted track radii greater than experimental ones. In [1], a phenomenological approach based on the TM concept was proposed to explain the evolution of track sizes with energy deposition for irradiated $\text{YBa}_2\text{Cu}_3\text{O}_{7-x}$ and $\text{Bi}_2\text{Sr}_2\text{CaCu}_2\text{O}_8$ superconductors. Although this model was successful in its design, it contained parameters independent on the physical properties of the materials and could be only considered as a preliminary investigation of the problem. A more detailed model of track formation in $\text{YBa}_2\text{Cu}_3\text{O}_{7-x}$ based on a system of coupled equations for electron and atom temperatures was proposed in [2, 3]. Our recent studies were devoted to further development of it.

ION DISSIPATION DYNAMICS. The radial distribution of dose around the path of a heavy ion was calculated in line with the delta-ray model of track structure, which is widespread in radiation dosimetry [4]. The model incorporates energy deposition due to primary excitations and ionization of atoms, and δ -electron kinetic energy transfer. According to it, the primary excitations contribute essentially, about 50%, in the region $r < 10$ nm. For $r > 10$ nm investment of δ -electrons entirely dominates. Since the radial distribution of dose cannot be regarded as instantaneous, at least for $t \geq 10$ fs when the thermal diffusivity of excited electron should be taken into account, a space-time dynamics of δ -electron energy deposition was formulated. This δ -electron dynamics, as the slowest one, was also used to find the moment when the energy deposition is stopped. We found that the most part of energy spent on track creation is released within the region $r < 1$ nm and $t < 0.15$ fs, although the process persists up to $t \sim 10^{-5}$ s and $r \sim 10^{-3}$ cm. Calculations show that δ -electron energy deposition at $r < 10$ nm comes to the end by the time of $t \sim 10$ fs. On the other hand, just by this moment Auger decays of all vacancies in the electron shells are expected to occur and thermodynamic equilibrium for the excited electrons to be established. Therefore, exactly the moment $t \simeq 10$ fs was taken as a proper initial time, when the basic equations of TS model may be used in a consistent manner with the radial distribution of dose at that moment estimated by the δ -electron dissipation dynamics.

DESCRIPTION OF THE ELECTRONIC SUBSYSTEM. The basic equations of TS model are nothing else but energy conservation laws which tolerate both quantum and

classical physical specifications implemented in thermal physical constants, particularly, in specific heat and thermal conductivity of electronic and atom subsystems. Thermal capacity of electrons in a wide temperature interval can be found numerically [5]

$$\rho C_e(T_e) = \int \varepsilon \frac{f(\varepsilon, T_e)}{dT_e} dn(\varepsilon),$$

where $f(\varepsilon, T_e)$ is the Fermi distribution, $dn(\varepsilon) = \eta(\varepsilon) d\varepsilon$, and $\eta(\varepsilon)$ is the electronic density of states. Calculated and an experimentally estimated value of Sommerfeld's parameter, $\gamma = \rho C_e/T_e$, is $(2.4 \pm 0.8) \cdot 10^{-4}$ J/(cm³ K²). The effective electron-atom relaxation time, $\tau = \rho C_e/g$, due to linear dependence of C_e on T_e , acquires the same linear form, $\tau = (\gamma/g) T_e \equiv \alpha T_e$, as it was predicted by Allen's theory [6], in which

$$\tau = \frac{\pi}{3} \frac{k_B}{\lambda' \langle \omega^2 \rangle} T_e.$$

Using the experimental value of $\lambda' \langle \omega^2 \rangle = 475 \pm 30$ meV², one can estimate parameter α from Allen's theory:

$$\alpha = (1.28 \pm 0.06) \cdot 10^{-16} \text{s/K}.$$

In such a way, electron-atom coupling g can be expressed through α and γ parameters: $g = \gamma/\alpha$. In fact, the following form of equation was found to be the most convenient for numerical solution:

$$\rho C_e(T_e) \frac{\partial T_e}{\partial t} = \frac{1}{r} \frac{\partial}{\partial r} \left[r D_e \rho C_e(T_e) \frac{\partial T_e}{\partial r} \right] - \frac{\rho C_e(T_e)}{\tau(T_e)} \cdot (T_e - T_i) + q(r, t), \quad (1)$$

where $q(r, t)$ is ion energy deposition described above.

DESCRIPTION OF THE ATOMIC SYSTEM. Utilization of electrons and atoms temperatures, T_e and T_i , in the TSM should not conceal the fact that true thermodynamic equilibrium states, either liquid or solid, are not expected to form during the period of energy excitation in the track. Therefore, the legality of usage of experimental values such as specific heat and heat of fusion, measured at thermodynamic equilibrium, formally accepted as the TS model parameters, is still doubtful. For instance, although the lattice temperature in the vicinity of ion's trajectory can exceed the melting temperature, it would be unrealistic suggesting peritectic reactions (usually taking place during melting of YBa₂Cu₃O_{7-x}) to occur during a picosecond time interval. In our calculations we accepted the traditional TSM estimation that energy expended on the amorphous track formation, Q_a , coincides with the heat Q_m necessary for melting of the lattice inside the track. For lattice thermal capacity, also usual Dulong-Petit value was taken. Thermal conductivity of atomic system, K_i , was chosen in accordance with existing experimental data, $K_i = 5.6 \times 10^{-2}$ J(s cm K)⁻¹. Since K_i is suggested to be temperature independent, thermal diffusivity $D_i = K_i/\rho C_i$ can be introduced and equation for the atomic system was taken in the following form:

$$\frac{\partial T_i}{\partial t} = D_i^{eff}(T_i) \Delta T_i + \frac{1}{\tau(T_e)} \frac{C_e(T_e)}{C_i^{eff}(T_i)} (T_e - T_i), \quad (2)$$

with functions $\tau(T_e)$, $C_e(T_e)$ defined in the previous section and

$$C_i^{eff} = C_i + Q_m \delta(T_m - T_i) \quad (3)$$

being the effective specific heat which includes the melting heat, $Q_m = 1.216$ kJ/g.

To solve numerically system (1) and (2), a *regularization* of C_i^{eff} and $D_i^{eff} = K_i/\rho C_i^{eff}$ was performed in neighborhood $T_m - \Delta \leq T_i \leq T_m + \Delta$ of melting temperature:

$$C_i^{eff}(T_i) = C_i + \frac{Q_f - 2C_i\Delta}{\sigma\sqrt{2\pi}} \exp\left(-\frac{(T_i - T_m)^2}{2\sigma^2}\right), \quad (4)$$

where $\sigma = 5$ K, $\Delta = 4.5 \sigma$.

NUMERICAL SOLUTION. Calculations were carried out on a grid of variables r and t with time and spatial steps h_t and h_r , respectively, $h_r = 0.025$ nm and $h_t = 2.5 \cdot 10^{-18}$ s. Source $q(r, t)$ was simulated before resolution of the system and retained for $r \in [0.1, 100.1]$ nm and $t \in [0, 5 \cdot 10^{-15}]$ s as a matrix of data at the same space-time grid. For numerical solution, the system of equations (1), (2) at internal mesh points was approximated by a difference scheme [7] with weights $\gamma \in [0, 1]$ and so was reduced to a system of linear algebraic ones. The difference scheme ensures the first order accuracy with respect to time for $\gamma \neq 0.5$. The explicit scheme, corresponding to $\gamma = 0$, is convergent only in case of $|h_t| < \frac{|h_r|^2}{2} \left(\frac{|\tilde{C}_e|}{|K_e|}\right)_{min}$ and $|\tilde{D}_i| |h_t| < |h_r|^2 / 2$, where \tilde{D}_i is a constant. This means that inequalities $h_r \gg h_t$ and $n_t \gg n_r$ should hold. Such restrictions make calculations computer time consuming. The implicit schemes ($\gamma \neq 0$) are absolutely convergent for every h_r and h_t and, therefore, are much more economical. In addition, the symmetrical implicit scheme ($\gamma = 0.5$) implemented in our calculations is absolutely convergent and has a second order accuracy with respect to both variables for not too small steps h_r and h_t .

DESCRIPTION OF TRACK RADII. Experimentally observed radii of tracks, r_{exp} , in $\text{YBa}_2\text{Cu}_3\text{O}_{7-x}$ single crystal with [001] axis oriented parallel to the incident ion beam are given in Table 1 along with results of our calculations.

Table 1: Experimentally observed radii of tracks, r_{exp} , in $\text{YBa}_2\text{Cu}_3\text{O}_{7-x}$ single crystal taken from [8] and results of their theoretical description. Pseudo-diffusivity of electrons, $D_e \equiv K_e/\rho C_e$, was taken to adjust the theoretical track radii to r_{exp} . Uncertainties for ^{129}Xe at 41 MeV/amu are due to getting respective values into the bifurcation region (see below).

Ion	Energy, MeV/amu	dE/dx, keV/nm	r_{exp} , nm	a , nm	D_e , cm ² /s
^{129}Xe	1.3	26.2	2-3	2.71	0.730
^{129}Xe	2.6	30	2.5	2.49	0.768
^{129}Xe	10	27.9	1.3	1.35	0.605
^{129}Xe	27	18.7	1.3	1.6	0.326
^{129}Xe	41	14.8	0.56	0.44-1.55	0.223-0.222
^{208}Pb	3.7	43.7	4	4.1	1.130
^{208}Pb	10	42.5	3	3.02	1.015
^{208}Pb	20	37	3.5	3.52	0.805
^{208}Pb	25	34.5	3	3.06	0.732

Dependence of obtained electron pseudo-diffusivity D_e on the energy deposition dE/dx is shown in Fig. 1 (a). Main sources of errors, visible as point scattering around the

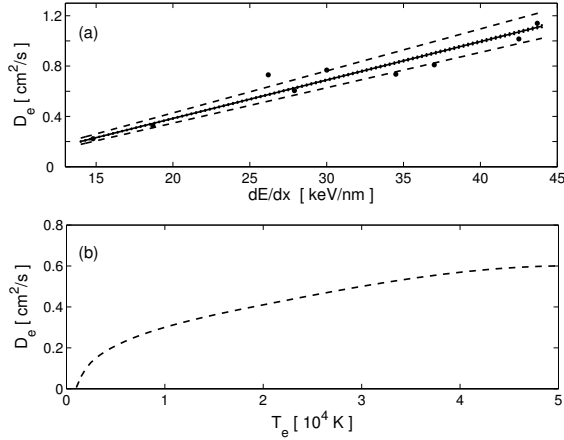


Figure 1: (a) Dependence of electron pseudo-diffusivity, D_e , on energy deposition in $\text{YBa}_2\text{Cu}_3\text{O}_{7-x}$ found using the thermal spike model (points). Straight solid line describes the smoothed relationship, dotted line demonstrates theoretical uncertainties resulting from experimental errors of parameter $\alpha = (1.3 \pm 0.1) \cdot 10^{-16} \text{ s/K}$. The role of the melting heat experimental errors represented by small “waves” along the solid line. (b) Theoretical $D_e(T_e)$ dependence for amorphous carbon extracted from [9]

solid line, are presumably fluctuation of experimental track radii (caused by thermal conductivity variations in different patterns) and inaccuracies of dE/dx . The figure gives a distinct evidence that parameter D_e for $\text{YBa}_2\text{Cu}_3\text{O}_{7-x}$ cannot be considered independent on the electron temperature, as it is supposed in the Caen version of TSM [10]. To speak in support of our conclusion, D_e as a function of T_e for amorphous carbon, calculated on the basis of theoretical results of [9], is shown in Fig. 1 (b). It is seen that for this case pseudo-diffusivity also increases essentially at electron temperatures $\sim 10^3 \text{ K}$, which are typical for track formation in $\text{YBa}_2\text{Cu}_3\text{O}_{7-x}$ too. But what is more important that the values of D_e established here turned out to be close indeed to the magnitude $D_e \simeq 1 \text{ cm}^2/\text{s}$ usually **assumed** in the Caen and some other track formation models. Therefore, we incline to consider the results of our theoretical estimations for this value to be realistic enough.

Comparison of the theoretical electron-atom relaxation time with results of femtosecond laser experiments [11, 12] is not as trivial as it may appear. Time of molten region formation, t_a , should not be confused with time of electron-atom relaxation, τ , although in the femtosecond laser experiments, where electrons get cold mainly due to local electron-atom interactions, they are in close agreement. Calculations have shown that in the case under consideration, due to influence of cold electrons at the boundary, the inequality $t_a \gg \tau$ takes place at the moment $t = t_a$. This is distinctly seen in Fig. 2 where $\tau(T_e)$ at the moving boundary of molten region is shown depending on time. On the other hand, the value of $\tau(T_e)$ at the moment of track formation is always of the same order as it have been approximately determined in femtosecond laser experiments [11, 12].

CONCLUDING REMARKS. It has been shown that TS model explains track formation in high- T_c superconductor $\text{YBa}_2\text{Cu}_3\text{O}_{7-x}$ in self-consistent manner without any free parameters. At the same time, high sensitivity of track radii to a small change of D_e (see [13, 14, 15]) requires a special investigation. We suppose that this problem can be

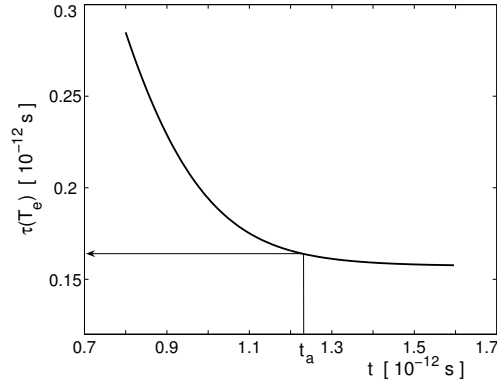


Figure 2: $\tau(T_e(a, t))$ distribution for ion ^{129}Xe at 2.6 MeV/amu in $\text{YBa}_2\text{Cu}_3\text{O}_{7-x}$

resolved by taking into account the so-called superheating which is possible due to very short duration of lattice excitation. Such phenomenon has been registered at similar (in many respect) femtosecond laser experiments. Theory cannot be considered as accomplished too without explanation of elliptic track formation corresponding to the case of irradiation along (100) and (010) directions.

References

- [1] *Szenes G.* // Phys. Rev. B, 1996-I, V. 54, P.12458.
- [2] *Goncharov I.N., Kostenko B.F., Philinova V.P.* // Phys. Lett. A. 2001. V.288. P.111.
- [3] *I.N. Goncharov, B.F. Kostenko, V.P. Philinova.* // J. of Comput. Meth. in Sci. and Eng. 2002. V. 2, p.169.
- [4] *Waligorski M.P.R., Hamm R.N., Katz R.* // Nucl. Tracks Radiat. Meas. 1986. V.1. P.309.
- [5] *Ayrjan E.A., Fedorov A.V., Kostenko B.F.* // Part. Nucl. Lett. 2000, V.99. P.42.
- [6] *Allen P.P. et al.* // Phys. Rev. B. 1994-I. V.49. P.9073.
- [7] *Pribish J.* // Ph.D. Thesis, JINR 11-2005-142, Dubna, 2005.
- [8] *Toulemonde M., Bouffard S., Studer E.* // Nucl. Instr. Meth. B. 1994. V.91. P.108.
- [9] *Schiwietz G. et al.* // Nucl. Instr. and Meth. B. 2000. V.164-165. P.354.
- [10] *Toulemonde M., Dufour C., Paumier E.* // Phys. Rev. B. 1992-II. V.46. P.14362.
- [11] *Brorson S.D. et al.* // Solid State Comm. 1990. V.74. P.1305.
- [12] *Vengrus I.I. et al.* // Pis'ma v JETP. 1995. V.62. P.739.
- [13] *B.F. Kostenko, J. Pribish, I.V. Puzynin.* // J. of Comput. Meth. in Sci. and Eng. (to be published).
- [14] *Kostenko B.F., Pribish J.* // Bulletin of Peoples' Friendship University of Russia, series - Applied and Computer Mathematics. 2005. V.4. p.55.
- [15] *Kostenko B.F., Pribish J., Goncharov I.N.* // Part. Nucl. Lett. 2006. V.3, 2006, p. 31.